

Fermionic Corrections to the Three-Loop Matching Coefficient of the Vector Current

P. Marquard^(a), J.H. Piclum^(a,b), D. Seidel^(a), M. Steinhauser^(a)

(a) Institut für Theoretische Teilchenphysik, Universität Karlsruhe (TH)

76128 Karlsruhe, Germany

(b) II. Institut für Theoretische Physik, Universität Hamburg

22761 Hamburg, Germany

Abstract

In this paper we consider the matching coefficient of the vector current between Quantum Chromodynamics (QCD) and Non-Relativistic QCD (NRQCD) to three-loop order in perturbation theory. We evaluate the fermionic corrections containing a closed massless fermion loop. The results are building blocks both for the bottom and top quark system at threshold. We explain in detail the methods used for the evaluation of the Feynman diagrams, classify the occurring master integrals and provide results for the latter. The numerical effects are significant. They have the tendency to improve the behaviour of the perturbative series — both for the bottom and top quark system.

PACS numbers: 12.38.Bx 14.65.Ha

1 Introduction

One of the main goals of a future international linear collider (ILC) is the precise measurement of the top quark threshold. Next to a precise extraction of the strong coupling an unrivaled determination of the top quark mass and its width is possible. This would open up a new chapter in the electroweak precision physics which leads to very strong checks of the Standard Model or possible extensions.

The theoretical calculations are based on an effective theory [1,2] (for a review see [3]) which enables the simultaneous expansion in the two small parameters present in threshold phenomena, the strong coupling α_s and the velocity of the heavy quarks, v . Furthermore, a resummation of correction terms like $(\alpha_s/v)^n$ to all orders is possible in perturbation theory. In a first step the effective theory is constructed in a matching procedure where it is required that the Green functions agree with the corresponding ones in full QCD in the limit of infinitely heavy top quark mass. In a second step the Green function in the effective theory has to be evaluated leading to the desired cross section.

Experimental studies [4] have shown that an uncertainty of less than 3% is necessary for the theoretical predictions for the cross section of the reaction $e^+e^- \rightarrow t\bar{t}$ in the threshold region, i.e. for $\sqrt{s} \approx 350$ GeV. This has not yet been achieved.

As far as the strong coupling is concerned currently the analysis is complete to next-to-next-to-leading order (NNLO) [5] demonstrating the urgent need for the third-order corrections. This huge enterprise has been started already some years ago and many building blocks have been evaluated starting from the determination of the third-order Hamiltonian [6], third-order corrections to the energy levels and wave functions [7–9] up to the evaluation of the contributions from the Coulomb potential to the non-relativistic Green function [9]. Next to fixed-order corrections also the resummation of next-to-next-to leading logarithmic terms has been considered and quite some progress has been achieved [10–13].

In order to reach a theory-uncertainty below 3% it is also necessary to worry about electroweak effects which can be parametrically as big as the third-order QCD terms. First results in this context are available [14,15] which show that indeed numerical effects in the region of a few percent are possible.

In this paper a further building block needed for the N³LO analysis is provided: the fermionic corrections to the matching coefficient of the vector current. More precisely we compute the three-loop contributions to the matching coefficient containing at least one closed loop of massless fermions which we enumerate by n_l .

The paper is organized as follows: in the next section we describe in detail the theoretical framework and the methods used for the calculation. In particular, we classify the occurring integrals and discuss their evaluation. Sections 3 and 4 contain a detailed discussion about the wave function and matching coefficient up to order $\alpha_s^3 n_l$, respectively. In Section 5 we briefly discuss the phenomenological impact of our result and Section 6 contains our conclusions and outlook. In the Appendix a complete list of master integrals is provided — both for the “natural” and the ϵ -finite basis.

2 Method

The matching coefficient establishing the relation between the quark current in the full and effective theory constitutes a building block for all threshold phenomena involving the coupling of a photon or Z boson to heavy quarks. We define the currents through

$$\begin{aligned} j_v^\mu &= \bar{Q}\gamma^\mu Q, \\ \tilde{j}^i &= \phi^\dagger \sigma^i \chi, \end{aligned} \tag{1}$$

and generically denote the heavy quark by Q . ϕ and χ are two-component Pauli spinors for quark and anti-quark, respectively. The definition of the matching coefficient is established through

$$j_v^k = c_v(\mu)\tilde{j}^k + \frac{d_v(\mu)}{6m_Q^2}\phi^\dagger\sigma^k\vec{D}^2\chi + \dots, \tag{2}$$

where $k = 1, 2, 3$ denotes the spacial components. \vec{D} contains the space-like components of the gauge-covariant derivative involving the gluon fields and the ellipsis stand for operators of higher mass dimension. The second term on the r.h.s. of Eq. (2) is already of NNLO with $d_v = 1 + \mathcal{O}(\alpha_s)$. The Wilson coefficients c_v and d_v may be expressed as series in α_s and represent the contributions from the hard modes which have been integrated out in order to arrive at the effective theory. Note that both the higher order terms in the inverse heavy quark mass and the time-like component is not of interest for the aim of this paper. The purpose of this paper is the evaluation of the fermionic correction to the non-singlet contribution of c_v containing at least one closed massless quark loop. The one-loop corrections to d_v contain no contribution proportional to n_f .

In order to compute c_v it is obvious to consider the $Q\bar{Q}\gamma$ vertex which in the following is denoted by Γ_v . This effectively transforms Eq. (2) into

$$Z_2\Gamma_v = c_v\tilde{Z}_2\tilde{Z}_v^{-1}\tilde{\Gamma}_v + \dots, \tag{3}$$

where we have on the left- and right-hand side quantities of the full and effective theory, respectively, and the ellipses denote terms suppressed by inverse powers of the heavy quark mass. In Eq. (3) it is understood that the couplings and masses in Γ_v are renormalized.

Since c_v takes into account the degrees of freedom which have been integrated out from the full theory it depends in our case only on α_s and — for dimensional reasons — on $\ln \mu^2/m_Q^2$. In particular, c_v does not explicitly depend on the momenta of the external particles. Thus, it is useful to apply the so-called threshold expansion [16, 17] to Eq. (3) which has the consequence that Γ_v has to be evaluated for $s = 4m_Q^2$ since all except the hard region cancel in Eq. (3). Furthermore, on the right-hand side only tree contributions have to be considered. In particular we have $\tilde{Z}_2 = 1$.

Starting from two-loop order the matching procedure exhibits infra-red divergences which are compensated by ultra-violet divergences of the effective theory rendering physical quantities finite. In Eq. (3) the renormalization constant \tilde{Z}_v which generates the

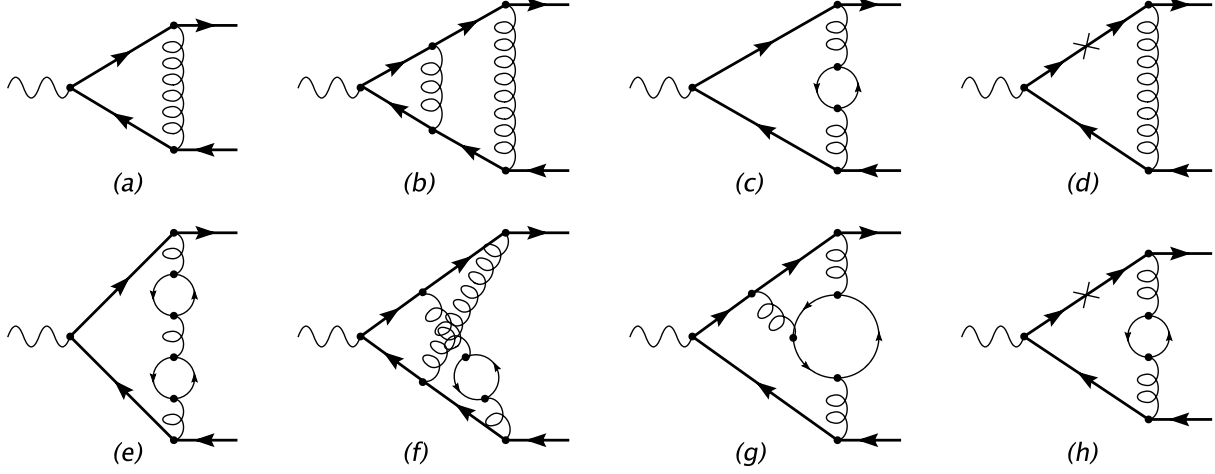


Figure 1: Feynman diagrams contributing to the matching coefficient. Bold lines denote heavy quarks with mass m_Q , thin lines denote massless quarks and curly lines denote gluons. In (d) and (h) mass counterterm diagrams are shown.

anomalous dimension of \tilde{j}_v takes over this part. Note that the vector current in the full theory does not get renormalized.

Sample Feynman diagrams contributing to the one-, two- and three-loop fermionic part of c_v are shown in Fig. 1. Due to the special kinematic situation with $s = q^2 = 4m_Q^2$ and on-shell heavy quark lines it is possible to perform a partial fractioning in the integrands corresponding to the various types of diagrams and map all occurring integrals to one of the following functions:

$$\begin{aligned}
J_{\pm}^{(2)}(n_1, \dots, n_5) &= \left(\frac{\mu^{2\epsilon}}{i\pi^{d/2}} \right)^2 \int \frac{d^d k \, d^d l}{(k^2)^{n_1} (l^2)^{n_2} ((k-l)^2)^{n_3} (k^2 + q \cdot k)^{n_4} (l^2 \pm q \cdot l)^{n_5}}, \\
L_{\pm}^{(2)}(n_1, \dots, n_5) &= \left(\frac{\mu^{2\epsilon}}{i\pi^{d/2}} \right)^2 \int \frac{d^d k \, d^d l}{(k^2)^{n_1} (l^2)^{n_2} ((k+l)^2 + q \cdot (k+l))^{n_3} (k^2 + q \cdot k)^{n_4} (l^2 \pm q \cdot l)^{n_5}}, \\
J_{\pm}^{(3)}(n_1, \dots, n_9) &= \left(\frac{\mu^{2\epsilon}}{i\pi^{d/2}} \right)^3 \int \frac{d^d k \, d^d l \, d^d p}{(k^2)^{n_1} (l^2)^{n_2} (p^2)^{n_3} ((k-l)^2)^{n_4} ((l-p)^2)^{n_5} ((p-k)^2)^{n_6} \\
&\quad \times \frac{(l^2 + q \cdot l)^{-n_8}}{(k^2 + q \cdot k)^{n_7} (p^2 \pm q \cdot p)^{n_9}}, \\
L_{\pm}^{(3, n_l)}(n_1, \dots, n_9) &= \left(\frac{\mu^{2\epsilon}}{i\pi^{d/2}} \right)^3 \int \frac{d^d k \, d^d l \, d^d p}{(k^2)^{n_1} (l^2)^{n_2} ((k+l)^2 + q \cdot (k+l))^{n_3} (k^2 + q \cdot k)^{n_4} \\
&\quad \times \frac{(p^2 + q \cdot p)^{-n_9}}{(l^2 \pm q \cdot l)^{n_5} (p^2)^{n_6} ((p+k)^2)^{n_7} ((p-l)^2)^{n_8}}. \tag{4}
\end{aligned}$$

For convenience we have also listed the two-loop functions $J_{\pm}^{(2)}$ and $L_{\pm}^{(2)}$ originally defined in Ref. [16]. The three-loop functions $J_{\pm}^{(3)}$ and $L_{\pm}^{(3, n_l)}$ contain irreducible scalar products

which are shown as numerators in the three-loop integrals in Eq. (4). The corresponding indices can only adopt values less or equal to zero. Furthermore, only two out of the three indices n_6 , n_7 and n_8 in $L_{\pm}^{(3,n_i)}$ can have positive values. Note that the integrals $J_+^{(2)}$, $L_+^{(2)}$ and $J_+^{(3)}$ are actually two-point functions whereas the integrals $J_-^{(2)}$, $L_-^{(2)}$, $J_-^{(3)}$ and $L_{\pm}^{(3,n_i)}$ correspond to vertices.

All Feynman diagrams are generated with `QGRAF` [18]. The various topologies are identified with the help of `q2e` and `exp` [19,20] which also adapts the notation in order to match the one of Eq. (4).

In a next step the reduction of the various functions to so-called master integrals has to be achieved. For this step we have chosen two approaches: the Laporta method [21,22] and Baikov's method [23,24] in the formulation of [25]. The application of these methods reduces the three-loop integrals to twelve master integrals. Since some of the master integrals are only known numerically it is very useful to construct a so-called ϵ -finite basis [26]. Details of this procedure and the results for the master integrals are given in Appendix A. Let us in the following provide more details on our implementation of each of the two reduction methods.

2.1 Implementation of the Laporta algorithm

The Laporta algorithm is based on the integration-by-parts (IBP) relations [27] where in a first step a huge system of equations is created by inserting numerical integer values into the relations. After assigning a weight specifying the complexity to each occurring integral the system of equations is solved step-by-step. In this way an arbitrary integral is expressed in terms of master integrals which cannot be further reduced.

To date there is only one publicly available computer code, `AIR` [28], where the Laporta algorithm is implemented. We have successfully applied `AIR` to the two-loop diagrams. However, the three-loop integrals of Eq. (4) cannot be treated with the help of `AIR`.

For this reason we have chosen to write a new implementation of Laporta's algorithm, `Crusher` [29]. It is written in `C++` and uses `GiNaC` [30] for simple manipulations like taking derivatives of polynomial quantities. In the practical implementation of the Laporta algorithm one of the most time-consuming operations is the simplification of the coefficients appearing in front of the individual integrals. This task is performed with the help of `Fermat` [31] where a special interface has been used (see Ref. [32]). The main features of the implementation are the automated generation of the IBP identities and a complete symmetrization of the diagrams. Using `Crusher` we solved approximately forty million equations to reduce all integrals to master integrals.

2.2 Baikov's method

Baikov's method is also based on the IBP relations. Here, however, one explicitly constructs the coefficient functions of the master integrals as parametric integrals over some polynomial, which encodes the topology of the initial integral. The integrations can then

be performed as Cauchy integrations around the origin or as contour integrations between the roots of the polynomial. The results are rational functions depending on the dimension and the kinematical invariants.

In some cases, however, it is not possible to perform the integrations in this way. In these cases one has to solve the integration-by-parts relations for the parametric integrals. They are similar to the relations for the initial integral, however, they depend on less indices and are thus in general significantly simpler. Since the relations can still be quite complicated, it is convenient to again use Laporta's algorithm. In the current calculation the program AIR was used for this task.

In order to perform the calculations, the algorithms for each integral were implemented in FORM [33]. In a first step, however, everything was implemented in Mathematica. This is very convenient since it is possible to produce almost all needed Mathematica code automatically. Once the program is finished, it can be easily translated to FORM and the Mathematica version can be used for debugging.

The two-loop calculation was done entirely with this method. In the three-loop case, however, it turned out that a complete solution of the recurrence relations for the coefficient functions is not possible with AIR. The calculation was therefore done with the Laporta method described above. We used Baikov's method only for the n_l^2 part and to cross-check some of the coefficient functions.

3 Wave function renormalization constant

According to Eq. (3) the wave function renormalization constant in the on-shell scheme Z_2 constitutes a crucial input for the computation of c_v . It has been computed to two- and three-loop approximation in Refs. [34] and [35], respectively. We have repeated the calculation of the two-loop and fermionic three-loop contributions which are needed for the present calculation and find complete agreement with the literature. For completeness we repeat the result for Z_2 which can be cast into the form

$$\begin{aligned}
Z_2 &= 1 + \frac{\alpha_s(\mu)}{\pi} \left(\frac{e^{\gamma_E}}{4\pi} \right)^{-\epsilon} \delta Z_2^{(1)} + \left(\frac{\alpha_s(\mu)}{\pi} \right)^2 \left(\frac{e^{\gamma_E}}{4\pi} \right)^{-2\epsilon} \delta Z_2^{(2)} \\
&\quad + \left(\frac{\alpha_s(\mu)}{\pi} \right)^3 \left(\frac{e^{\gamma_E}}{4\pi} \right)^{-3\epsilon} \left(\delta Z_2^{(3,nl)} + \text{non-}n_l \text{ terms} \right) + \mathcal{O}(\alpha_s^4), \quad (5)
\end{aligned}$$

with

$$\begin{aligned}
\delta Z_2^{(1)} &= -C_F \left[\frac{3}{4\epsilon} + 1 + \frac{3}{4}L_\mu + \left(2 + \frac{1}{16}\pi^2 + L_\mu + \frac{3}{8}L_\mu^2 \right) \epsilon \right. \\
&\quad \left. + \left(4 + \frac{1}{12}\pi^2 - \frac{1}{4}\zeta(3) + \left(2 + \frac{1}{16}\pi^2 \right) L_\mu + \frac{1}{2}L_\mu^2 + \frac{1}{8}L_\mu^3 \right) \epsilon^2 \right], \quad (6)
\end{aligned}$$

$$\begin{aligned}
\delta Z_2^{(2)} = & \left[\frac{11}{32\epsilon^2} - \frac{127}{192\epsilon} - \frac{1705}{384} + \frac{5}{16}\pi^2 - \frac{1}{2}\pi^2 \ln 2 + \frac{3}{4}\zeta(3) - \frac{215}{96}L_\mu - \frac{11}{32}L_\mu^2 \right. \\
& + \left(-\frac{9907}{768} + \frac{769}{1152}\pi^2 - \frac{23}{8}\pi^2 \ln 2 + \pi^2 \ln^2 2 + \frac{129}{16}\zeta(3) - \frac{7}{40}\pi^4 + \frac{1}{2}\ln^4 2 + 12a_4 \right. \\
& \left. + \left(-\frac{2057}{192} + \frac{109}{192}\pi^2 - \pi^2 \ln 2 + \frac{3}{2}\zeta(3) \right) L_\mu - \frac{259}{96}L_\mu^2 - \frac{11}{32}L_\mu^3 \right] C_A C_F \\
& + \left[\frac{9}{32\epsilon^2} + \left(\frac{51}{64} + \frac{9}{16}L_\mu \right) \frac{1}{\epsilon} + \frac{433}{128} - \frac{49}{64}\pi^2 + \pi^2 \ln 2 - \frac{3}{2}\zeta(3) + \frac{51}{32}L_\mu + \frac{9}{16}L_\mu^2 \right. \\
& + \left(\frac{211}{256} - \frac{339}{128}\pi^2 + \frac{23}{4}\pi^2 \ln 2 - 2\pi^2 \ln^2 2 - \frac{297}{16}\zeta(3) + \frac{7}{20}\pi^4 - \ln^4 2 - 24a_4 \right. \\
& \left. + \left(\frac{433}{64} - \frac{49}{32}\pi^2 + 2\pi^2 \ln 2 - 3\zeta(3) \right) L_\mu + \frac{51}{32}L_\mu^2 + \frac{3}{8}L_\mu^3 \right] C_F^2 \\
& + \left[\left(\frac{1}{16} + \frac{1}{4}L_\mu \right) \frac{1}{\epsilon} + \frac{947}{288} - \frac{5}{16}\pi^2 + \frac{11}{24}L_\mu + \frac{3}{8}L_\mu^2 + \left(\frac{17971}{1728} - \frac{445}{288}\pi^2 \right. \right. \\
& \left. \left. + 2\pi^2 \ln 2 - \frac{85}{12}\zeta(3) + \left(\frac{1043}{144} - \frac{29}{48}\pi^2 \right) L_\mu + \frac{5}{8}L_\mu^2 + \frac{7}{24}L_\mu^3 \right) \epsilon \right] C_F T \\
& + \left[-\frac{1}{8\epsilon^2} + \frac{11}{48\epsilon} + \frac{113}{96} + \frac{1}{12}\pi^2 + \frac{19}{24}L_\mu + \frac{1}{8}L_\mu^2 + \right. \\
& \left. + \left(\frac{851}{192} + \frac{127}{288}\pi^2 + \zeta(3) + \left(\frac{145}{48} + \frac{3}{16}\pi^2 \right) L_\mu + \frac{23}{24}L_\mu^2 + \frac{1}{8}L_\mu^3 \right) \epsilon \right] C_F T n_l \quad (7)
\end{aligned}$$

and

$$\begin{aligned}
\delta Z_2^{(3,n_l)} = & C_F T n_l \left\{ \left[\frac{11}{72\epsilon^3} - \frac{169}{432\epsilon^2} + \left(\frac{313}{1296} + \frac{1}{4}\zeta(3) \right) \frac{1}{\epsilon} \right. \right. \\
& + \frac{111791}{15552} + \frac{13}{48}\pi^2 + \frac{47}{36}\pi^2 \ln 2 - \frac{2}{9}\pi^2 \ln^2 2 - \frac{35}{72}\zeta(3) + \frac{19}{1080}\pi^4 - \frac{1}{9}\ln^4 2 - \frac{8}{3}a_4 \\
& + \left. \left(\frac{169}{27} - \frac{1}{18}\pi^2 + \frac{1}{3}\pi^2 \ln 2 + \frac{1}{4}\zeta(3) \right) L_\mu + \frac{469}{288}L_\mu^2 + \frac{11}{72}L_\mu^3 \right] C_A \\
& + \left[\frac{3}{32\epsilon^3} + \left(-\frac{19}{192} + \frac{3}{32}L_\mu \right) \frac{1}{\epsilon^2} + \left(-\frac{235}{384} - \frac{7}{128}\pi^2 - \frac{1}{4}\zeta(3) - \frac{41}{64}L_\mu - \frac{3}{64}L_\mu^2 \right) \frac{1}{\epsilon} \right. \\
& - \frac{3083}{2304} + \frac{2845}{2304}\pi^2 - \frac{47}{18}\pi^2 \ln 2 + \frac{4}{9}\pi^2 \ln^2 2 + \frac{473}{96}\zeta(3) - \frac{229}{2160}\pi^4 + \frac{2}{9}\ln^4 2 + \frac{16}{3}a_4 \\
& + \left. \left(-\frac{1475}{384} + \frac{133}{384}\pi^2 - \frac{2}{3}\pi^2 \ln 2 + \frac{1}{4}\zeta(3) \right) L_\mu - \frac{179}{128}L_\mu^2 - \frac{11}{64}L_\mu^3 \right] C_F \\
& + \left[\left(\frac{1}{36} + \frac{1}{12}L_\mu \right) \frac{1}{\epsilon^2} + \left(-\frac{5}{216} + \frac{1}{144}\pi^2 - \frac{1}{9}L_\mu + \frac{1}{24}L_\mu^2 \right) \frac{1}{\epsilon} \right. \\
& - \frac{4721}{1296} + \frac{19}{54}\pi^2 - \frac{1}{36}\zeta(3) + \left. \left(-\frac{329}{108} + \frac{25}{144}\pi^2 \right) L_\mu - \frac{7}{12}L_\mu^2 - \frac{5}{72}L_\mu^3 \right] T \\
& + \left[-\frac{1}{36\epsilon^3} + \frac{11}{216\epsilon^2} + \frac{5}{1296\epsilon} - \frac{5767}{7776} - \frac{19}{108}\pi^2 - \frac{7}{18}\zeta(3) \right. \\
& \left. - \left(\frac{167}{216} + \frac{1}{18}\pi^2 \right) L_\mu - \frac{19}{72}L_\mu^2 - \frac{1}{36}L_\mu^3 \right] T n_l \left. \right\}, \tag{8}
\end{aligned}$$

where $L_\mu = \ln(\mu^2/m_Q^2)$, $C_F = (N_c^2 - 1)/(2N_c)$, $C_A = N_c$, $T = 1/2$ and $n_l = n_f - 1$ is the number of light-quark flavours. $N_c = 3$ and α_s is the strong coupling renormalized in the $\overline{\text{MS}}$ scheme with n_f active flavours. $\zeta(3)$ is Riemann's ζ function with the value $\zeta(3) = 1.202057\dots$, γ_E is Euler's constant with the value $\gamma_E = 0.577216\dots$ and $a_4 = \text{Li}_4(1/2) = 0.517479\dots$. Note that $\delta Z_2^{(1)}$ and $\delta Z_2^{(2)}$ are given to order ϵ^2 and ϵ , respectively, which is needed for the three-loop calculation of c_v .

The integrals needed for Z_2 constitute a subset of the ones needed for c_v . In fact, from Eq. (4) only the integral types with a “+” sign contribute. We also want to mention that our calculation poses the first independent check of the n_l part of Ref. [35].

4 Matching coefficient

It is convenient to cast the perturbative expansion of the matching coefficient in the form

$$c_v = 1 + \frac{\alpha_s(\mu)}{\pi} c_v^{(1)} + \left(\frac{\alpha_s(\mu)}{\pi} \right)^2 c_v^{(2)} + \left(\frac{\alpha_s(\mu)}{\pi} \right)^3 c_v^{(3)} + \mathcal{O}(\alpha_s^4), \tag{9}$$

where the one- [36] and two-loop [37, 38] (see also Ref. [39]) terms are given by

$$\begin{aligned}
c_v^{(1)} &= -2C_F \\
c_v^{(2)} &= \left(-\frac{151}{72} + \frac{89}{144}\pi^2 - \frac{5}{6}\pi^2 \ln 2 - \frac{13}{4}\zeta(3) \right) C_A C_F \\
&\quad + \left(\frac{23}{8} - \frac{79}{36}\pi^2 + \pi^2 \ln 2 - \frac{1}{2}\zeta(3) \right) C_F^2 + \left(\frac{22}{9} - \frac{2}{9}\pi^2 \right) C_F T \\
&\quad + \frac{11}{18} C_F T n_l - \frac{1}{2} \left[4\beta_0 + \pi^2 \left(\frac{1}{2}C_A + \frac{1}{3}C_F \right) \right] C_F \ln \frac{\mu^2}{m_Q^2}, \tag{10}
\end{aligned}$$

with $\beta_0 = (11C_A/3 - 4Tn_f/3)/4$. Note that the terms proportional to $\beta_0 \ln \frac{\mu^2}{m_Q^2}$ are connected to the choice $\alpha_s(\mu)$ in Eq. (9) whereas the ones proportional to $\pi^2 \ln \frac{\mu^2}{m_Q^2}$ originate from the separation of hard and soft scales in the construction of NRQCD.

The decomposition of $c_v^{(3)}$ according to the colour structures is given by

$$c_v^{(3)} = C_F T n_l (C_{FCFFL} + C_{ACFAL} + T_{CFHL} + T_{n_l C_{FLL}}) + \text{non-}n_l \text{ terms.} \tag{11}$$

In the notation of Eq. (3) it is understood that in Γ_v the renormalization of the coupling constant and heavy quark mass is already performed. The renormalization of the coupling constant can be done straightforwardly by replacing the bare coupling with the renormalization constant times the renormalized coupling. The mass renormalization, however, is more intricate since we are dealing with on-shell integrals. It is therefore convenient to calculate the counterterms directly by considering one- and two-loop diagrams with zero-momentum insertions in the massive fermion lines. Sample diagrams are shown in Fig. 1(d) and (h). The vertex denoted by a cross is replaced by the mass renormalization constant in the on-shell scheme. One-loop diagrams with two insertions are not needed at the order considered in this paper.

Starting from three-loop level the wave function renormalization constant begins to depend on the QCD gauge parameter, ξ [35]. However, it is interesting to note that the colour structures entering our result (cf. Eq. (8)) are independent of ξ . As a consequence the quantity Γ_v also has to be independent of ξ which is indeed the case in our calculation. Actually, the ξ dependence remaining in the sum of all genuine three-loop diagrams contributing to Γ_v is canceled by the contribution where a two-loop mass counterterm is inserted in the one-loop vertex diagram (cf. Fig. 1(d)). Note that the mass counterterm contribution from the two-loop fermionic diagram (cf. Fig. 1(h)) is ξ independent. The cancellation of the gauge parameter serves as a welcome check for the correctness of our result.

As already mentioned above, after taking into account all counterterm contributions there are still infra-red divergences left in the quantity $Z_2 \Gamma_v$ and thus in $c_v \tilde{Z}_v^{-1}$. This is a consequence of the threshold expansion accompanied by dimensional regularization which is used to extract the matching coefficient. Alternatively it would have been possible to choose a cut-off for the momentum integrations which finally results in a factorization scale

separating the hard and soft momenta. In our approach the infra-red poles are absorbed into \tilde{Z}_v which we define in the $\overline{\text{MS}}$ scheme. As a consequence the matching coefficient itself is finite but scale dependent. In the physical quantities this scale dependence gets canceled against the corresponding contributions from the effective theory. Of course, one has to make sure that for the subtraction of the poles in the effective theory the same scheme is used as in the full theory.

For the renormalization constant \tilde{Z}_v we obtain

$$\begin{aligned}\tilde{Z}_v &= 1 + \left(\frac{\alpha_s(\mu)}{\pi}\right)^2 \left(\frac{1}{12}C_F^2 + \frac{1}{8}C_F C_A\right) \frac{\pi^2}{\epsilon} \\ &+ \left(\frac{\alpha_s(\mu)}{\pi}\right)^3 C_F T n_l \left[\left(\frac{1}{54}C_F + \frac{1}{36}C_A\right) \frac{\pi^2}{\epsilon^2} - \left(\frac{25}{324}C_F + \frac{37}{432}C_A\right) \frac{\pi^2}{\epsilon} \right] \\ &+ \dots ,\end{aligned}\tag{12}$$

where the ellipses stand for non- n_l and $\mathcal{O}(\alpha_s^4)$ terms.

Our final result for $c_v^{(3)}$ reads

$$\begin{aligned}c_{FFL} &= 46.7(1) + \left(-\frac{17}{12} + \frac{61}{36}\pi^2 - \frac{2}{3}\pi^2 \ln 2 + \frac{1}{3}\zeta(3)\right) L_\mu + \frac{1}{18}\pi^2 L_\mu^2, \\ c_{FAL} &= 39.6(1) + \left(\frac{181}{54} - \frac{67}{432}\pi^2 + \frac{5}{9}\pi^2 \ln 2 + \frac{13}{6}\zeta(3)\right) L_\mu + \left(\frac{11}{9} + \frac{1}{12}\pi^2\right) L_\mu^2, \\ c_{FHL} &= -\frac{557}{162} + \frac{26}{81}\pi^2 + \left(-\frac{55}{27} + \frac{4}{27}\pi^2\right) L_\mu - \frac{4}{9}L_\mu^2, \\ c_{FLL} &= -\frac{163}{162} - \frac{4}{27}\pi^2 - \frac{11}{27}L_\mu - \frac{2}{9}L_\mu^2.\end{aligned}\tag{13}$$

The uncertainties assigned to the numerical constants in c_{FFL} and c_{FAL} are based on a conservative estimate. Note that the precision of these quantities is more than enough for all phenomenological applications. Inserting the numerical values for the colour factors we obtain for $\mu = m_Q$

$$c_v^{(3)} \approx -0.823 n_l^2 + 121. n_l + \text{non-}n_l \text{ terms} .\tag{14}$$

The coefficients in Eq. (13) correspond to an expansion parameter $\alpha_s(\mu)$, as given in Eq. (9). Choosing instead $\alpha_s(m_Q)$ leads to

$$\begin{aligned}\bar{c}_{FFL} &= 46.7(1) + \frac{25}{108}\pi^2 L_\mu - \frac{1}{18}\pi^2 L_\mu^2, \\ \bar{c}_{FAL} &= 39.6(1) + \frac{37}{144}\pi^2 L_\mu - \frac{1}{12}\pi^2 L_\mu^2, \\ \bar{c}_{FHL} &= -\frac{557}{162} + \frac{26}{81}\pi^2, \\ \bar{c}_{FLL} &= -\frac{163}{162} - \frac{4}{27}\pi^2.\end{aligned}\tag{15}$$

The dependence on L_μ in Eq. (15) is canceled against contributions from the effective theory. They agree with the ones of Ref. [40]¹.

5 Phenomenological applications

Let us in this section estimate the numerical effect of our new terms on the bottom and top system. In particular we consider the decay of the $\Upsilon(1S)$ bound state to leptons and the production of top quark pairs close to threshold.

Next to the matching coefficient considered in the previous Sections a crucial ingredient for these quantities is the wave function at the origin. Currently the second order is known completely [41–45] and at order α_s^3 the quadratically [46,47] and linearly [12,40] enhanced logarithms and the corrections proportional to β_0^3 [8,9] are available. It is convenient to introduce the quantity $\rho_1 = |\psi_1(0)|^2/|\psi_1^C(0)|^2$ where the Coulomb wave function is given by $|\psi_n^C(0)|^2 = C_F^3 \alpha_s^3 m_q^3 / (8\pi n^3)$. Let us for completeness list the results for principle quantum number $n = 1$

$$\begin{aligned} \rho_1 = & 1 + \frac{\alpha_s(\mu_s)}{\pi} \left[\left(4 - \frac{2}{3}\pi^2 \right) \beta_0 + \frac{3}{4}a_1 \right] \\ & + \left(\frac{\alpha_s(\mu_s)}{\pi} \right)^2 \left\{ \left[-C_A C_F + \left(-2 + \frac{2}{3}S(S+1) \right) C_F^2 \right] \pi^2 \ln(C_F \alpha_s(\mu_s)) \right. \\ & + \left(-\frac{5}{3}\pi^2 + 20\zeta(3) + \frac{1}{9}\pi^4 \right) \beta_0^2 + \left(4 - \frac{2}{3}\pi^2 \right) \beta_1 + \left(\frac{5}{2} - \frac{2}{3}\pi^2 \right) \beta_0 a_1 \\ & + \left. \frac{3}{16}a_1^2 + \frac{3}{16}a_2 + \frac{9}{4}\pi^2 C_A C_F + \left(\frac{33}{8} - \frac{13}{9}S(S+1) \right) \pi^2 C_F^2 \right\} \\ & + \left(\frac{\alpha_s(\mu_s)}{\pi} \right)^3 \left\{ \pi^2 \mathcal{C}_2 \ln^2(C_F \alpha_s(\mu_s)) + \pi^2 \mathcal{C}_1 \ln(C_F \alpha_s(\mu_s)) + \mathcal{C}_0^{\beta_0^3} + \dots \right\}, \quad (16) \end{aligned}$$

with

$$\begin{aligned} \mathcal{C}_2 = & \left(-2C_A C_F + \left(-4 + \frac{4}{3}S(S+1) \right) C_F^2 \right) \beta_0 - \frac{2}{3}C_A^2 C_F \\ & + \left(-\frac{41}{12} + \frac{7}{12}S(S+1) \right) C_A C_F^2 - \frac{3}{2}C_F^3, \quad (17) \end{aligned}$$

¹Note that in Ref. [40] there is a typo in the coefficient of the L_μ^2 term. The “ $-3/2$ ” should read “ $+1$ ”.

$$\begin{aligned}
\mathcal{C}_1 = & \left[\left(-3 + \frac{2}{3}\pi^2 \right) C_A C_F + \left(\frac{4}{3}\pi^2 - \left(\frac{10}{9} + \frac{4}{9}\pi^2 \right) S(S+1) \right) C_F^2 \right] \beta_0 \\
& + \left[-\frac{3}{4} C_A C_F + \left(-\frac{9}{4} + \frac{2}{3} S(S+1) \right) C_F^2 \right] a_1 + \frac{1}{4} C_A^3 + \left(\frac{59}{36} - 4 \ln 2 \right) C_A^2 C_F \\
& + \left(\frac{143}{36} - 4 \ln 2 - \frac{19}{108} S(S+1) \right) C_A C_F^2 + \left(-\frac{35}{18} + 8 \ln 2 - \frac{1}{3} S(S+1) \right) C_F^3 \\
& + \left(-\frac{32}{15} + 2 \ln 2 + (1 - \ln 2) S(S+1) \right) C_F^2 T + \frac{49}{36} C_A C_F T n_l \\
& + \left(\frac{8}{9} - \frac{10}{27} S(S+1) \right) C_F^2 T n_l \tag{18}
\end{aligned}$$

and

$$\begin{aligned}
\mathcal{C}_0^{\beta_0^3} = & \beta_0^3 \left[-20 + \frac{22}{3}\pi^2 + 112\zeta(3) - \frac{7}{5}\pi^4 - 12\pi^2\zeta(3) - 40\zeta(5) - 16\zeta(3)^2 \right. \\
& \left. + \frac{4}{105}\pi^6 \right], \tag{19}
\end{aligned}$$

where $\mu_s = C_F m_q \alpha_s(\mu_s)$ is the soft scale. It is straightforward to obtain the result for general $\alpha_s(\mu)$ using standard renormalization group analyses. In Eqs. (16)–(18) S is the spin quantum number which is equal to one in our applications. The ellipses in Eq. (16) represent yet unknown corrections like, e.g., the pure ultrasoft contributions.

For completeness we provide the one- and two-loop coefficients of the β function and the static potential which are given by

$$\begin{aligned}
\beta_0 &= \frac{1}{4} \left(\frac{11}{3} C_A - \frac{4}{3} T n_l \right), \\
\beta_1 &= \frac{1}{16} \left(\frac{34}{3} C_A^2 - \frac{20}{3} C_A T n_l - 4 C_F T n_l \right), \\
a_1 &= \frac{31}{9} C_A - \frac{20}{9} T n_l, \\
a_2 &= \left(\frac{4343}{162} + 4\pi^2 + \frac{22}{3}\zeta(3) - \frac{1}{4}\pi^4 \right) C_A^2 - \left(\frac{1798}{81} + \frac{56}{3}\zeta(3) \right) C_A T n_l \\
&\quad - \left(\frac{55}{3} - 16\zeta(3) \right) C_F T n_l + \left(\frac{20}{9} T n_l \right)^2. \tag{20}
\end{aligned}$$

5.1 Bottom system

The leptonic decay of the $\Upsilon(1S)$ state can be cast in the form [41–45]

$$\Gamma(\Upsilon(1S) \rightarrow l^+ l^-) = \Gamma^{\text{LO}} \rho_1 \left[c_v^2(m_b) + \frac{C_F^2 \alpha_s^2(\mu_s)}{12} c_v(m_b) (d_v(m_b) + 3) \right] + \dots, \tag{21}$$

with $\Gamma^{\text{LO}} = 4\pi N_c Q_b^2 \alpha^2 |\psi_1^C(0)|^2 / (3m_b^2)$, $Q_b = -1/3$, $N_c = 3$, α is Sommerfeld's fine-structure constant and nonperturbative contributions to Eq. (21) are ignored.

Inserting the perturbative expansion for ρ_1 and c_v we obtain

$$\begin{aligned} \Gamma_1 \approx & \Gamma_1^{\text{LO}} (1 - 1.70 \alpha_s(m_b) - 7.98 \alpha_s^2(m_b) + 30.0 \alpha_s^3(m_b)|_{n_l} + \dots) \\ & \times \left[1 - 0.30 \alpha_s(\mu_s) + \alpha_s^2(\mu_s) (17.2 - 5.19 \ln \alpha_s(\mu_s)) \right. \\ & \left. + \alpha_s^3(\mu_s) \left(-14.4 \ln^2 \alpha_s(\mu_s) + 0.17 \ln \alpha_s(\mu_s) - 34.9 |_{\beta_0^3} \right) + \dots \right], \end{aligned} \quad (22)$$

where in the matching coefficient $\mu = m_b$ has been chosen and the corresponding strong coupling is defined with five and $\alpha_s(\mu_s)$ with four active flavours.

Starting from $\alpha_s(M_Z) = 0.118$ we have used the program `RunDec` [48] to obtain $\alpha_s(m_b) = 0.2096$ and $\alpha_s(\mu_s) = 0.2967$ with $m_b = 5.3$ GeV and $\mu_s = 2.0967$ GeV which leads to

$$\Gamma_1 \approx \Gamma_1^{\text{LO}} (1 - 0.446_{\text{NLO}} + 1.75_{\text{NNLO}} - 1.20_{\text{N}^3\text{LO}'} + \dots), \quad (23)$$

where Eq. (22) is expanded and terms of order α_s^4 are dropped consistently. The prime reminds that the third-order corrections are not complete. Apart from the new contribution to c_v and the known third-order corrections to ρ_1 we have also included all interference terms which are proportional to powers of n_l . Note that the new corrections are responsible for the reduction of $\text{N}^3\text{LO}'$ terms from -1.67 to -1.20 which amounts to about 47% of the Born cross section. However, in total the fermionic corrections tend to further reduce the strong increase of the perturbative coefficients leading to an overall correction factor of approximately 10%.

We have performed the numerical analysis also for $m_b = 4.8$ GeV. There are changes in the individual contributions to Γ_1 (c.f. Eq. (23)) of the order of a few per cent, however, the final correction factor remains the same.

5.2 Top system

In the top-quark case, the nonperturbative effects are negligible. However, the effect of the top-quark total decay width Γ_t has to be properly taken into account [49], as it is relatively large and smears out the Coulomb-like resonances below threshold. The NNLO analysis of the cross section [5] shows that only the ground-state pole gives rise to a prominent resonance.

A crucial quantity in connection to the threshold production of top quark pairs is the peak of the normalized cross section $R = \sigma(e^+e^- \rightarrow t\bar{t})/\sigma(e^+e^- \rightarrow \mu^+\mu^-)$. It is dominated by the contribution from the would-be toponium ground-state, which can be cast in the form

$$R_1(e^+e^- \rightarrow t\bar{t}) = R_1^{\text{LO}} \rho_1 \left[c_v^2(m_t) + \frac{C_F^2 \alpha_s^2(\mu_s)}{12} c_v(m_t) (d_v(m_t) + 3) \right] + \dots, \quad (24)$$

with the leading order term $R_1^{\text{LO}} = 6\pi N_c Q_t^2 |\psi_1^C(0)|^2 / (m_t^2 \Gamma_t)$. The contributions from the higher Coulomb-like poles and the continuum are not included in Eq. (24).

The analog equations to Eqs. (22) and (23) read

$$\begin{aligned}
R_1 \approx & R_1^{\text{LO}} (1 - 1.70 \alpha_s(m_t) - 7.89 \alpha_s^2(m_t) + 37.2 \alpha_s^3(m_t)|_{\text{n}_1} + \dots) \\
& \times \left[1 - 0.43 \alpha_s(\mu_s) + \alpha_s^2(\mu_s) (16.1 - 5.19 \ln \alpha_s(\mu_s)) \right. \\
& \left. + \alpha_s^3(\mu_s) \left(-13.8 \ln^2 \alpha_s(\mu_s) + 2.06 \ln \alpha_s(\mu_s) - 27.2 |_{\beta_0^3} \right) + \dots \right], \quad (25)
\end{aligned}$$

where $\alpha_s(m_t)$ and $\alpha_s(\mu_s)$ are defined with six and five active flavours, respectively. Using again $\alpha_s(M_Z) = 0.118$ one gets $\alpha_s(m_t) = 0.1075$ and $\alpha_s(\mu_s) = 0.1398$ with $m_t = 175$ GeV and $\mu_s = 32.625$ GeV and finally

$$R_1 \approx R_1^{\text{LO}} (1 - 0.243_{\text{NLO}} + 0.435_{\text{NNLO}} - 0.195_{\text{N}^3\text{LO}} + \dots). \quad (26)$$

The fermionic corrections to c_v are responsible for a reduction of the third-order coefficient from -0.268 to -0.195 and thus amount to moderate 7% of the leading order term. Similarly as for the bottom quark case also for the top quark the perturbative series is alternating and the third-order coefficient tends to stabilize the expansion. It is interesting to note that after the inclusion of our new terms the total corrections amount to less than 1%.

6 Conclusions and outlook

This paper deals with the question of establishing a relation for the vector current between full QCD and NRQCD. The corresponding matching coefficient, c_v , constitutes a building block in all threshold phenomena involving a vector coupling. The main result of this paper is the fermionic three-loop contribution to c_v which contains a closed light fermion loop. The numerical effect of the new terms is relatively big and amounts to about 47% for the bottom and to about 7% for the top quark system. However, their inclusion leads to a reduction of the overall corrections. E.g., in the case of the top quark the corrections to the normalization at the peak of the production cross section amount to less than 1% after including all currently known perturbative terms.

Several steps still have to be taken in order to arrive at the complete analysis of the top-anti-top quark system at threshold. Next to the non-fermionic pieces to c_v the major building blocks which are still missing are the ultra-soft corrections and the three-loop static potential.

Acknowledgements

We would like to thank A.A. Penin and V.A. Smirnov for useful comments and discussions. J.H.P. would like to thank S. Bekavac for discussions about Mellin-Barnes integrals and M. Kalmykov for useful advice on two-loop sunset integrals. We thank M. Tentyukov for providing the interface to `Fermat`. This work was supported by the ‘‘Impuls- und Vernetzungsfonds’’ of the Helmholtz Association, contract number VH-NG-008 and by the DFG through SFB/TR 9. The Feynman diagrams were drawn with `JaxoDraw` [50]

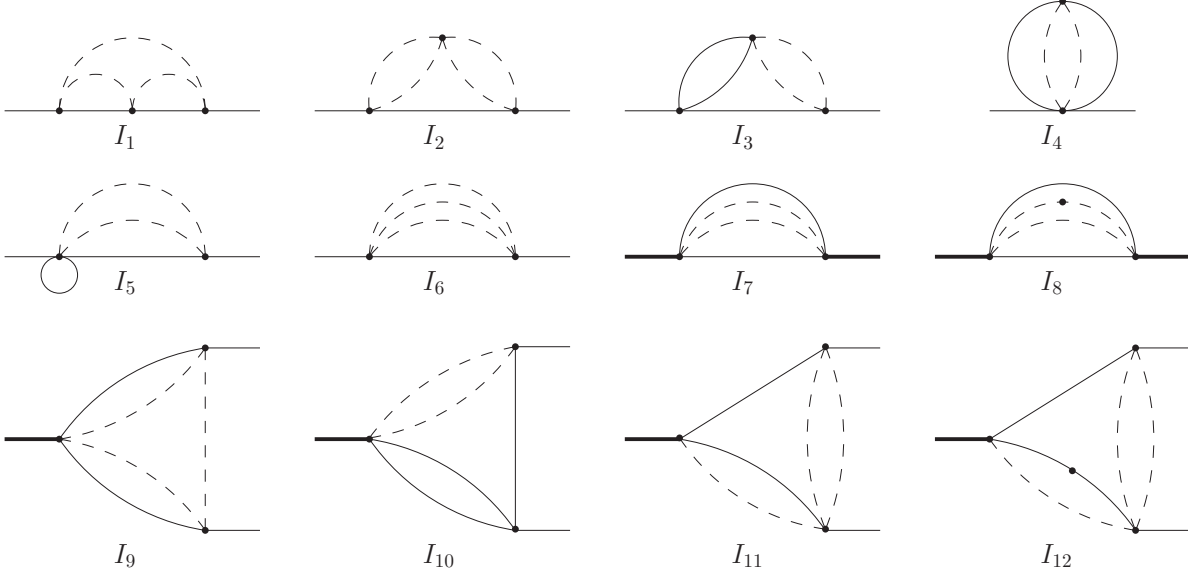


Figure 2: Three-loop master integrals. Bold lines denote massive lines with mass $2m_Q$, thin lines denote massive lines with mass m_Q and dashed lines denote massless lines. All external lines are on-shell. A dot on a line denotes a squared propagator.

A Results for the master integrals

The master integrals for the three-loop functions of Eq. (4) are shown in Fig. 2. For the self-energy integrals I_1 – I_6 the external momentum squared equals the square of the heavy quark mass, $q^2 = m_Q^2$. For the integrals I_7 and I_8 we have $q^2 = 4m_Q^2$. The momenta q_1 and q_2 flowing out of the vertex diagrams on the right fulfill $q_1^2 = q_2^2 = m_Q^2$ with $(q_1 + q_2)^2 = 4m_Q^2$. In Minkowski space the results for the master integrals read

$$\begin{aligned}
I_1 &= J_+^{(3)}(0, 1, 0, 1, 1, 0, 1, 0, 1) \\
&= m_Q^2 \left(\frac{\mu^2}{m_Q^2} e^{-\gamma_E} \right)^{3\epsilon} \left\{ \frac{1}{3\epsilon^3} + \frac{5}{3\epsilon^2} + \left(4 + \frac{3}{4}\pi^2 \right) \frac{1}{\epsilon} - \frac{10}{3} + \frac{11}{4}\pi^2 + \frac{25}{3}\zeta(3) \right. \\
&\quad + \left(-\frac{302}{3} + 2\pi^2 + \frac{89}{3}\zeta(3) + \frac{3059}{1440}\pi^4 \right) \epsilon + \left(-734 - \frac{69}{2}\pi^2 + 16\zeta(3) + \frac{9751}{1440}\pi^4 \right. \\
&\quad \left. \left. + \frac{107}{4}\pi^2\zeta(3) + \frac{2309}{5}\zeta(5) \right) \epsilon^2 + \mathcal{O}(\epsilon^3) \right\}, \tag{27}
\end{aligned}$$

$$\begin{aligned}
I_2 &= J_+^{(3)}(0, 1, 1, 1, 0, 1, 1, 0, 0) \\
&= -m_Q^2 \left(\frac{\mu^2}{m_Q^2} \right)^{3\epsilon} \frac{\Gamma^4(1-\epsilon)\Gamma^2(\epsilon)}{\Gamma^2(2-2\epsilon)} \frac{\Gamma(3\epsilon-1)\Gamma(3-6\epsilon)}{\Gamma(3-4\epsilon)}, \tag{28}
\end{aligned}$$

$$\begin{aligned}
I_3 &= L_+^{(3,m_l)}(0, 0, 1, 1, 1, 1, 0, 1, 0) \\
&= m_Q^2 \left(\frac{\mu^2}{m_Q^2} e^{-\gamma_E} \right)^{3\epsilon} \left\{ \frac{2}{3\epsilon^3} + \frac{10}{3\epsilon^2} + \left(\frac{26}{3} + \frac{1}{2}\pi^2 \right) \frac{1}{\epsilon} + 2 + \frac{9}{2}\pi^2 + \frac{14}{3}\zeta(3) \right. \\
&\quad + \left(-\frac{398}{3} + \frac{53}{2}\pi^2 - 16\pi^2 \ln 2 + \frac{238}{3}\zeta(3) + \frac{287}{720}\pi^4 \right) \epsilon + \left(-1038 + \frac{259}{2}\pi^2 \right. \\
&\quad \left. - 160\pi^2 \ln 2 + \frac{128}{3}\pi^2 \ln^2 2 + \frac{1862}{3}\zeta(3) + \frac{323}{720}\pi^4 + \frac{7}{2}\pi^2\zeta(3) + \frac{478}{5}\zeta(5) \right. \\
&\quad \left. + \frac{64}{3} \ln^4 2 + 512a_4 \right) \epsilon^2 + \mathcal{O}(\epsilon^3) \left. \right\}, \tag{29}
\end{aligned}$$

$$\begin{aligned}
I_4 &= J_+^{(3)}(0, 0, 0, 1, 1, 0, 1, 0, 1) \\
&= m_Q^4 \left(\frac{\mu^2}{m_Q^2} \right)^{3\epsilon} \frac{\Gamma^2(1-\epsilon)\Gamma(\epsilon)\Gamma^2(2\epsilon-1)\Gamma(3\epsilon-2)}{\Gamma(4\epsilon-2)\Gamma(2-\epsilon)}, \tag{30}
\end{aligned}$$

$$\begin{aligned}
I_5 &= J_+^{(3)}(0, 1, 0, 1, 0, 0, 1, 0, 1) \\
&= m_Q^4 \left(\frac{\mu^2}{m_Q^2} \right)^{3\epsilon} \Gamma(\epsilon-1) \frac{\Gamma^2(1-\epsilon)\Gamma(\epsilon)}{\Gamma(2-2\epsilon)} \frac{\Gamma(2\epsilon-1)\Gamma(3-4\epsilon)}{\Gamma(3-3\epsilon)}, \tag{31}
\end{aligned}$$

$$\begin{aligned}
I_6 &= J_+^{(3)}(0, 0, 1, 1, 1, 0, 1, 0, 0) \\
&= m_Q^4 \left(\frac{\mu^2}{m_Q^2} \right)^{3\epsilon} \frac{\Gamma^3(1-\epsilon)\Gamma(2\epsilon-1)\Gamma(3\epsilon-2)\Gamma(5-6\epsilon)}{\Gamma(3-3\epsilon)\Gamma(4-4\epsilon)}, \tag{32}
\end{aligned}$$

$$\begin{aligned}
I_7 &= J_-^{(3)}(0, 0, 0, 1, 1, 0, 1, 0, 1) \\
&= m_Q^4 \left(\frac{\mu^2}{m_Q^2} e^{-\gamma_E} \right)^{3\epsilon} \left\{ \frac{1}{3\epsilon^3} + \frac{1}{2\epsilon^2} + \left(-\frac{17}{36} + \frac{1}{12}\pi^2 \right) \frac{1}{\epsilon} - 6.6827387(1) \right. \\
&\quad \left. - 56.300353(1)\epsilon - 209.48231(1)\epsilon^2 + \mathcal{O}(\epsilon^3) \right\}, \tag{33}
\end{aligned}$$

$$\begin{aligned}
I_8 &= J_-^{(3)}(0, 0, 0, 2, 1, 0, 1, 0, 1) \\
&= -m_Q^2 \left(\frac{\mu^2}{m_Q^2} e^{-\gamma_E} \right)^{3\epsilon} \left\{ \frac{1}{3\epsilon^3} + \frac{2}{3\epsilon^2} + \left(-\frac{8}{3} + \frac{5}{6}\pi^2 \right) \frac{1}{\epsilon} + 10.797602(1) \right. \\
&\quad \left. + 62.250613(1)\epsilon + \mathcal{O}(\epsilon^2) \right\}, \tag{34}
\end{aligned}$$

$$\begin{aligned}
I_9 &= J_-^{(3)}(0, 1, 0, 1, 1, 0, 1, 0, 1) \\
&= m_Q^2 \left(\frac{\mu^2}{m_Q^2} e^{-\gamma_E} \right)^{3\epsilon} \left\{ \frac{1}{3\epsilon^3} + \frac{5}{3\epsilon^2} + \left(\frac{10}{3} + \frac{3}{4}\pi^2 \right) \frac{1}{\epsilon} + 33.8328(4) + 152.870(4)\epsilon \right. \\
&\quad \left. + \mathcal{O}(\epsilon^2) \right\}, \tag{35}
\end{aligned}$$

$$\begin{aligned}
I_{10} &= L_+^{(3,n_l)}(0, 0, 1, 1, 1, 0, 1, 1, 0) \\
&= m_Q^2 \left(\frac{\mu^2}{m_Q^2} e^{-\gamma_E} \right)^{3\epsilon} \left\{ \frac{2}{3\epsilon^3} + \frac{10}{3\epsilon^2} + \left(8 + \frac{1}{2}\pi^2 \right) \frac{1}{\epsilon} + 52.5698(4) + 145.087(4)\epsilon \right. \\
&\quad \left. + 562.250(14)\epsilon^2 + \mathcal{O}(\epsilon^3) \right\}, \tag{36}
\end{aligned}$$

$$\begin{aligned}
I_{11} &= J_-^{(3)}(0, 1, 0, 1, 0, 1, 1, 0, 1) \\
&= m_Q^2 \left(\frac{\mu^2}{m_Q^2} e^{-\gamma_E} \right)^{3\epsilon} \left\{ \frac{1}{2\epsilon^3} + \frac{11}{6\epsilon^2} + \left(-\frac{1}{6} + \frac{29}{24}\pi^2 \right) \frac{1}{\epsilon} + 34.791(4) + 154.08(2)\epsilon \right. \\
&\quad \left. + \mathcal{O}(\epsilon^2) \right\}, \tag{37}
\end{aligned}$$

$$\begin{aligned}
I_{12} &= J_-^{(3)}(0, 1, 0, 1, 0, 1, 1, 0, 2) \\
&= \left(\frac{\mu^2}{m_Q^2} e^{-\gamma_E} \right)^{3\epsilon} \left\{ \frac{1}{6\epsilon^3} + \frac{1}{2\epsilon^2} + \left(\frac{1}{6} + \frac{7}{24}\pi^2 \right) \frac{1}{\epsilon} + 7.024(4) + 32.04(2)\epsilon \right. \\
&\quad \left. + \mathcal{O}(\epsilon^2) \right\}, \tag{38}
\end{aligned}$$

where $\zeta(5) = 1.036927\dots$ and $a_4 = \text{Li}_4(1/2) = 0.517479\dots$

I_1 was calculated in Ref. [35]. We have repeated the calculation described in the reference with the program `XSummer` [51] and find complete agreement. The results for I_3 – I_6 can be found in Ref. [21]. We have checked the result for I_3 numerically with the help of a one-fold Mellin-Barnes [52, 53] representation and find complete agreement. Note, that I_2, I_4, I_5 and I_6 are quite simple to evaluate and are available for general ϵ . Nevertheless the result for I_6 as given in Ref. [35] is not correct whereas the correct result can be found in Ref. [21]. The pole part of I_7 agrees with the result of Ref. [54].

The remaining master integrals, I_7 – I_{12} , have been evaluated with the help of the Mellin-Barnes method where the evaluation of the integrals has been performed with the program `MB` [55]. I_7 and I_8 can be expressed in terms of a one-fold Mellin-Barnes representation and are thus known with a quite high precision. On the other hand, I_{10} is represented by a two-fold and I_9, I_{11} and I_{12} even by a three-fold integration which results in less accurate results. The quoted uncertainties in the above equations correspond to twice the Vegas error given by `MB` for the multi-dimensional integrals and to a conservative estimate in case of the one-dimensional integrals I_7 and I_8 . Note that the latter errors are negligible.

As can be seen in the above results some of the master integrals are needed to higher order in ϵ which on one hand makes the calculation very tedious and on the other hand leads to less accurate results. For this reason we decided to change basis and switch — at least for some of the integrals — to the so-called ϵ -finite master integrals [26] which have the advantage that the coefficient function is finite and thus the integral itself is only needed to order ϵ^0 .

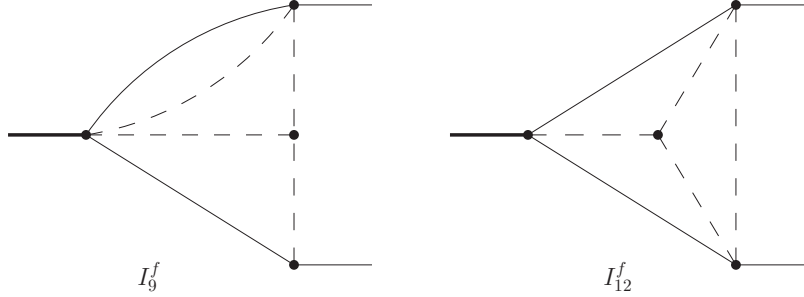


Figure 3: ϵ -finite master integrals. The same coding as in Fig. 2 is adopted.

Since I_1 – I_6 are known analytically, a replacement is, of course, not necessary. Furthermore, for I_7 and I_8 the numerical precision is sufficient for our calculation. As far as the remaining four integrals are concerned, we found it convenient to replace I_9 and I_{12} by the integrals shown in Fig. 3. Their numerical evaluation with the help of MB is straightforward leading to the results

$$\begin{aligned}
 I_9^f &= J_-^{(3)}(0, 1, 1, 1, 1, 0, 1, 0, 1) \\
 &= \left(\frac{\mu^2}{m_Q^2} e^{-\gamma_E} \right)^{3\epsilon} \left\{ \frac{1}{6\epsilon^3} + \frac{3}{2\epsilon^2} + \left(\frac{55}{6} + \frac{3}{8}\pi^2 \right) \frac{1}{\epsilon} + 64.678(8) + \mathcal{O}(\epsilon) \right\}, \quad (39)
 \end{aligned}$$

$$I_{12}^f = J_-^{(3)}(0, 1, 0, 1, 1, 1, 1, 0, 1) = \left(\frac{\mu^2}{m_Q^2} e^{-\gamma_E} \right)^{3\epsilon} \left\{ \frac{2.4041(4)}{\epsilon} + 8.1(2) + \mathcal{O}(\epsilon) \right\}. \quad (40)$$

Switching from I_9 and I_{12} to I_9^f and I_{12}^f reduces the number of coefficients which are only known numerically from 17 to 14. In particular the $1/\epsilon$ -poles of I_9 and I_{12} have been determined in analytical form from the ϵ -finite integrals via the corresponding IBP relations.

A further reduction is achieved after exploiting the locality and incorporating the knowledge of the linear $\ln(\mu^2/m_Q^2)$ term in c_v [40] which we have checked numerically in a first step. In this way the analytical result for the $1/\epsilon$ -pole of I_{11} has been determined. In total ten (eleven) numerical coefficients contribute to our final result given in Eqs. (13) and (14) using the ϵ -finite (“normal”) basis.

In the end it turned out, that the numerical precision is better using the “normal” basis. The reason is, that the uncertainty of the ϵ^0 -coefficient of I_{12}^f is by far the largest. Still, it was useful to consider the ϵ -finite basis since it enabled us to determine analytical results for two integral coefficients of the “normal” basis.

References

- [1] W. E. Caswell and G. P. Lepage, Phys. Lett. B **167** (1986) 437.

- [2] G. T. Bodwin, E. Braaten and G. P. Lepage, Phys. Rev. D **51** (1995) 1125 [Erratum-
ibid. D **55** (1997) 5853] [arXiv:hep-ph/9407339].
- [3] N. Brambilla *et al.*, arXiv:hep-ph/0412158.
- [4] M. Martinez and R. Miquel, Eur. Phys. J. C **27** (2003) 49 [arXiv:hep-ph/0207315].
- [5] A. H. Hoang *et al.*, Eur. Phys. J. directC **2** (2000) 1 [arXiv:hep-ph/0001286].
- [6] B. A. Kniehl, A. A. Penin, V. A. Smirnov and M. Steinhauser, Nucl. Phys. B **635**
(2002) 357 [arXiv:hep-ph/0203166].
- [7] A. A. Penin and M. Steinhauser, Phys. Lett. B **538** (2002) 335
[arXiv:hep-ph/0204290].
- [8] A. A. Penin, V. A. Smirnov and M. Steinhauser, Nucl. Phys. B **716** (2005) 303
[arXiv:hep-ph/0501042].
- [9] M. Beneke, Y. Kiyo and K. Schuller, Nucl. Phys. B **714** (2005) 67
[arXiv:hep-ph/0501289].
- [10] A. Pineda, Phys. Rev. D **65** (2002) 074007 [arXiv:hep-ph/0109117].
- [11] A. Pineda, Phys. Rev. D **66** (2002) 054022 [arXiv:hep-ph/0110216].
- [12] A. H. Hoang, Phys. Rev. D **69** (2004) 034009 [arXiv:hep-ph/0307376].
- [13] A. A. Penin, A. Pineda, V. A. Smirnov and M. Steinhauser, Nucl. Phys. B **699** (2004)
183 [arXiv:hep-ph/0406175].
- [14] A. H. Hoang and C. J. Reisser, Phys. Rev. D **71** (2005) 074022
[arXiv:hep-ph/0412258].
- [15] D. Eiras and M. Steinhauser, arXiv:hep-ph/0605227.
- [16] M. Beneke and V. A. Smirnov, Nucl. Phys. B **522** (1998) 321 [arXiv:hep-ph/9711391].
- [17] V. A. Smirnov, “Applied asymptotic expansions in momenta and masses,” Springer
(2002).
- [18] P. Nogueira, J. Comput. Phys. **105** (1993) 279.
- [19] R. Harlander, T. Seidensticker and M. Steinhauser, Phys. Lett. B **426** (1998) 125
[hep-ph/9712228].
- [20] T. Seidensticker, hep-ph/9905298.
- [21] S. Laporta and E. Remiddi, Phys. Lett. B **379** (1996) 283 [arXiv:hep-ph/9602417].
- [22] S. Laporta, Int. J. Mod. Phys. A **15** (2000) 5087 [arXiv:hep-ph/0102033].

- [23] P. A. Baikov, Phys. Lett. B **385** (1996) 404 [arXiv:hep-ph/9603267].
- [24] P. A. Baikov, Nucl. Instrum. Meth. A **389** (1997) 347 [arXiv:hep-ph/9611449].
- [25] V. A. Smirnov and M. Steinhauser, Nucl. Phys. B **672** (2003) 199 [arXiv:hep-ph/0307088].
- [26] K. G. Chetyrkin, M. Faisst, C. Sturm and M. Tentyukov, Nucl. Phys. B **742** (2006) 208 [arXiv:hep-ph/0601165].
- [27] K. G. Chetyrkin and F. V. Tkachov, Nucl. Phys. B **192** (1981) 159.
- [28] C. Anastasiou and A. Lazopoulos, JHEP **0407** (2004) 046 [arXiv:hep-ph/0404258].
- [29] P. Marquard and D. Seidel, unpublished.
- [30] C. Bauer, A. Frink and R. Kreckel, arXiv:cs.sc/0004015.
- [31] R. H. Lewis, Fermat's User Guide, <http://www.bway.net/~lewis>.
- [32] M. Tentyukov and J. A. M. Vermaseren, arXiv:cs.sc/0604052.
- [33] J. A. M. Vermaseren, arXiv:math-ph/0010025.
- [34] D. J. Broadhurst, N. Gray and K. Schilcher, Z. Phys. C **52** (1991) 111.
- [35] K. Melnikov and T. van Ritbergen, Nucl. Phys. B **591** (2000) 515 [arXiv:hep-ph/0005131].
- [36] G. Källen and A. Sarby, K. Dan. Vidensk. Selsk. Mat.-Fis. Medd. 29, N17 (1955) 1.
- [37] A. Czarnecki and K. Melnikov, Phys. Rev. Lett. **80** (1998) 2531 [arXiv:hep-ph/9712222].
- [38] M. Beneke, A. Signer and V. A. Smirnov, Phys. Rev. Lett. **80** (1998) 2535 [arXiv:hep-ph/9712302].
- [39] B. A. Kniehl, A. Onishchenko, J. H. Piclum and M. Steinhauser, Phys. Lett. B **638** (2006) 209 [arXiv:hep-ph/0604072].
- [40] B. A. Kniehl, A. A. Penin, M. Steinhauser and V. A. Smirnov, Phys. Rev. Lett. **90** (2003) 212001 [Erratum-ibid. **91** (2003) 139903(E)] [arXiv:hep-ph/0210161].
- [41] J. H. Kühn, A. A. Penin and A. A. Pivovarov, Nucl. Phys. B **534** (1998) 356 [arXiv:hep-ph/9801356].
- [42] A. A. Penin and A. A. Pivovarov, Phys. Lett. B **435** (1998) 413 [arXiv:hep-ph/9803363].

- [43] A. A. Penin and A. A. Pivovarov, Nucl. Phys. B **549** (1999) 217 [arXiv:hep-ph/9807421].
- [44] A. A. Penin and A. A. Pivovarov, Nucl. Phys. B **550** (1999) 375 [arXiv:hep-ph/9810496].
- [45] K. Melnikov and A. Yelkhovsky, Phys. Rev. D **59** (1999) 114009 [arXiv:hep-ph/9805270].
- [46] B. A. Kniehl and A. A. Penin, Nucl. Phys. B **577** (2000) 197 [arXiv:hep-ph/9911414].
- [47] A. V. Manohar and I. W. Stewart, Phys. Rev. D **63** (2001) 054004 [arXiv:hep-ph/0003107].
- [48] K. G. Chetyrkin, J. H. Kühn and M. Steinhauser, Comput. Phys. Commun. **133** (2000) 43 [arXiv:hep-ph/0004189].
- [49] V. S. Fadin and V. A. Khoze, JETP Lett. **46** (1987) 525 [Pisma Zh. Eksp. Teor. Fiz. **46** (1987) 417].
- [50] D. Binosi and L. Theussl, Comput. Phys. Commun. **161** (2004) 76 [arXiv:hep-ph/0309015].
- [51] S. Moch and P. Uwer, Comput. Phys. Commun. **174** (2006) 759 [arXiv:math-ph/0508008].
- [52] V. A. Smirnov, Phys. Lett. B **460** (1999) 397 [arXiv:hep-ph/9905323].
- [53] J. B. Tausk, Phys. Lett. B **469** (1999) 225 [arXiv:hep-ph/9909506].
- [54] S. Groote, J. G. Körner and A. A. Pivovarov, Eur. Phys. J. C **36** (2004) 471 [arXiv:hep-ph/0403122].
- [55] M. Czakon, arXiv:hep-ph/0511200.